

# A 2000-year lipid biomarker record preserved in a stalagmite from north-west Scotland



ALISON J. BLYTH,<sup>1,2\*</sup> ANDY BAKER,<sup>3</sup> LOUISE E. THOMAS<sup>4</sup> and PETER VAN CALSTEREN<sup>4</sup>

<sup>1</sup>School of Civil Engineering and Geosciences, Drummond Building, Newcastle University, Newcastle Upon Tyne, UK

<sup>2</sup>Department of Earth & Environmental Sciences, The Open University, Milton Keynes, UK

<sup>3</sup>Water Research Laboratory, School of Civil and Environmental Engineering, University of New South Wales, Manly Vale, New South Wales, Australia

<sup>4</sup>NERC Uranium-series Dating Facility, Department of Earth & Environmental Sciences, The Open University, Milton Keynes, UK

Received 9 July 2009; Revised 28 September 2010; Accepted 3 October 2010

**ABSTRACT:** Previous studies on lipid biomarkers preserved in Chinese stalagmites have indicated that ratios of low-molecular-weight (LMW) to high-molecular-weight (HMW) *n*-alkanes, *n*-alkan-2-ones, *n*-alkanols and *n*-alkanoic acids can be used as an index of vegetation versus microbial organic matter input to the system and, by extension, a marker of climatic changes, with increases in the proportion of LMW compounds coinciding with colder periods. Here we test whether this hypothesis is equally applicable to a different geographical region (north-west Scotland), by examining a stalagmite record of the past 200 years, and a wider range of lipid markers. We also test the applicability of other lipid proxies in this context, including the use of *n*-alkane ratios, to interpret vegetation changes, and unsaturated alkanolic acid ratios as climatic indicators. The results show that lipid proxies preserved in stalagmites, and especially those related to vegetation, are potentially extremely useful in palaeoenvironmental research. Of particular value is the use of  $C_{27}/C_{31}$  *n*-alkane ratios as a proxy for vegetation change, clearly indicating variations between herbaceous and arboreal cover. This proxy has now been successfully applied to samples from diverse environments, and can be considered sufficiently robust to be of use in analysing future stalagmite records. It will be of particular value in areas where reliable pollen records are not available, as is often the case with deeper cave deposits. However, the division between LMW and HMW aliphatic compounds is not a clear-cut case of microbial versus plant activity, with the changes in LMW compounds relating more closely to those in their HMW analogues than in specific bacterial biomarkers. The use of unsaturated alkanolic acid ratios here gives conflicting results, with the observed variation through time depending on the isomer measured. The discrepancies between the findings of this study and previous work are likely to be due to the varying controls on the lipids (original organic matter input, and compound degradation), which in turn will be affected by whether the main climatic limiting factor on the soil is temperature or precipitation. This suggests that lipid proxies preserved in stalagmites must be interpreted with care, particularly in the case of bacterial compounds which may be derived from within the cave or from the soil. However, many of these issues can be resolved by the use of multi-proxy studies. Copyright © 2011 John Wiley & Sons, Ltd.

**KEYWORDS:** biomarkers; climate; lipids; speleothem; stalagmites; vegetation.

## Introduction

Lipid biomarkers preserved in speleothems have been shown to have considerable potential as palaeoenvironmental proxies (Blyth *et al.*, 2008), with studies indicating relationships with palaeoclimatic conditions (Xie *et al.*, 2003, 2005), microbial communities (Blyth & Frisia, 2008; Huang *et al.*, 2008) and vegetational parameters (Blyth *et al.*, 2007). This is of value to Quaternary research for several reasons. A new proxy for vegetation change provides a complementary technique to existing approaches such as pollen analysis and can be utilised when conditions for pollen deposition or preservation are not favourable. This is often the case in caves, especially those that are relatively deep or have only small surface openings, yet caves and stalagmites in particular are excellent archives for palaeoenvironmental records, with stable isotope analyses of stalagmite calcite in particular being very well established as recorders of global and continental climate (for a review, see McDermott, 2004). The development of an organic record in stalagmites, recording changes in soil conditions and vegetation, is therefore of substantial interest as it can be compared directly with isotope-derived climatic records (albeit at a lower temporal resolution) recovered from the same sample. This will enable investigation of the rates and response of past

environments to climate change within a single context and without the need to match separately dated records. The strong dating control that can be achieved in stalagmites using U–Th series dating is also advantageous compared with many other sorts of terrestrial records.

However, although these techniques clearly have potential, they have not yet been applied to samples from a diverse range of geographical areas and environmental contexts. Therefore, it is difficult to judge whether these approaches are valid globally, or are environment-specific.

Here we apply a range of lipid parameters to a stalagmite deposited during the last 2 ka in Scotland. Xie *et al.* (2003) proposed that ratios of low-molecular-weight (LMW) to high-molecular-weight (HMW) *n*-alkanols and *n*-alkan-2-ones preserved in stalagmites recorded fluctuations in the relative amounts of plant and microbial input, driven by climatic (and particularly temperature) variations. Ratios of LMW/HMW *n*-alkanes did not correlate so well, but the alkane carbon number distribution was proposed as reflecting changes between herbaceous plant- and tree-dominated vegetational regimes. This latter contention was supported by Blyth *et al.* (2007), who identified changes in the ratios of  $C_{27}/C_{31}$  *n*-alkanes related to known vegetation clearances in a 100-year-old sample from Ethiopia. Alkanolic acids have also been proposed as being of significance. Xie *et al.* (2005) suggested that ratios of unsaturated to saturated microbial acids could reflect temperature changes, with lower temperatures resulting in a higher concentration of unsaturated acids due to twin mechanisms

\* Correspondence: A. J. Blyth, Department of Earth & Environmental Sciences, The Open University, Milton Keynes MK7 6AA, UK.  
E-mail: a.blyth@open.ac.uk

of slower degradation and increased production. Blyth *et al.* (2007) proposed that relative increases in HMW *n*-alkanoic acids could reflect the amount of plant matter input.

One of the issues that could interfere with these proxies is whether the LMW *n*-alkanoic acids, *n*-alkanols and *n*-alkanes do actually represent bacterial communities, and the HMW compounds represent vegetation input, or whether they have a more generalised and complex origin. To investigate this in our sample, 3-hydroxy acids, and branched LMW fatty acids, more specific bacterial biomarkers that have already been identified in stalagmites (Blyth *et al.*, 2006; Huang *et al.*, 2008), were also measured, as were known vegetation-specific sterols.

## Methods and materials

### Sample and site

Lower Traligill Cave is one of a number of caves developed in the Cambro-Ordovician Durness Limestone of the Traligill river valley, situated at the head of Loch Assynt in north-west Scotland (Dowswell, 1988; Fig. 1). Lower Traligill Cave is formed by two interconnecting series of passages developed along the strike plane of the Traligill Main Thrust (Dowswell, 1988). An active stream flows through the lower passages, while the upper series are dry, containing speleothem deposits fed by meteoric water from above. The area has a maritime climate, with annual precipitation of >1900 mm (Baker *et al.*, 1999), and a mean annual temperature of 7.2 °C. The basin upstream from the cave is primarily covered by peatland, the blanket mire being dominated by *Calluna*, *Erica* and Cyperaceae, with discontinuous areas of *Sphagnum* cover (Charman

*et al.*, 2001). However, the immediate area around the cave is principally overlain by thin mineral soils, supporting *Calluna* and grasses. Peat core analysis upstream suggests that the vegetation regime in the area has persisted for at least the last 3 ka, although prior to 1 ka, birch woodland was also a major component (Charman *et al.*, 2001).

The sample, Tral-1, was collected from the upper passages of the cave in December 2003. The stalagmite measures 75 mm in height, and is visibly laminated throughout the section with cream and brown calcite at a millimetre scale (Fig. 2). Under UV microscopy regular and near-continuous laminae can be seen throughout the stalagmite body (from the base to a hiatus in the top 5 mm), demonstrating a seasonal connection to the soil organic matter pool. However, although the sample was being actively fed by drip-water when collected, and so is assumed to be modern at the surface, under microscopic inspection, it becomes apparent that the outer series of laminae (subsample A) contain a number of hiatuses, preventing the body of the stalagmite from being dated by laminae counting relative to the present day.

This specific site and sample were chosen because the area is known to provide stalagmites amenable to U–Th dating and with very low detrital thorium levels. An additional bonus is the presence of comparative peat records for the time period of interest. Tral-1 was considered especially suitable for the work due to its clear lamination, making sectioning into logical and coherent units easy.

### U–Th dating

To provide a temporal framework for the analyses, the sample was dated by six uranium series dates taken at intervals through the stalagmite body (Fig. 2). Analyses were carried out at the NERC-OU-Uranium Series Facility laboratories at the Open University (UK): speleothem samples (typically 0.5 g) were totally dissolved and spiked with a mixed  $^{229}\text{Th}/^{236}\text{U}$  spike. Uranium and thorium fractions were separated on 2-mL anion exchange columns using standard techniques (Edwards *et al.*, 1987).

Both uranium and thorium fractions were diluted to approximately 10 p.p.b. and then run on a Nu Instruments Multi-Collector Inductively Coupled Plasma Mass Spectrometer (MC-ICPMS) (Turner *et al.*, 1996). A dynamic peak-switching routine was employed measuring  $^{234}\text{U}/^{236}\text{U}$  and  $^{235}\text{U}/^{236}\text{U}$  (a proxy for  $^{238}\text{U}$ , assuming a  $^{238}\text{U}/^{235}\text{U}$  natural ratio of 137.88) and separately for  $^{230}\text{Th}/^{229}\text{Th}$  and  $^{232}\text{Th}/^{229}\text{Th}$ . Although  $^{232}\text{Th}$  abundance is not required for the age calculation it is always measured so that we can monitor

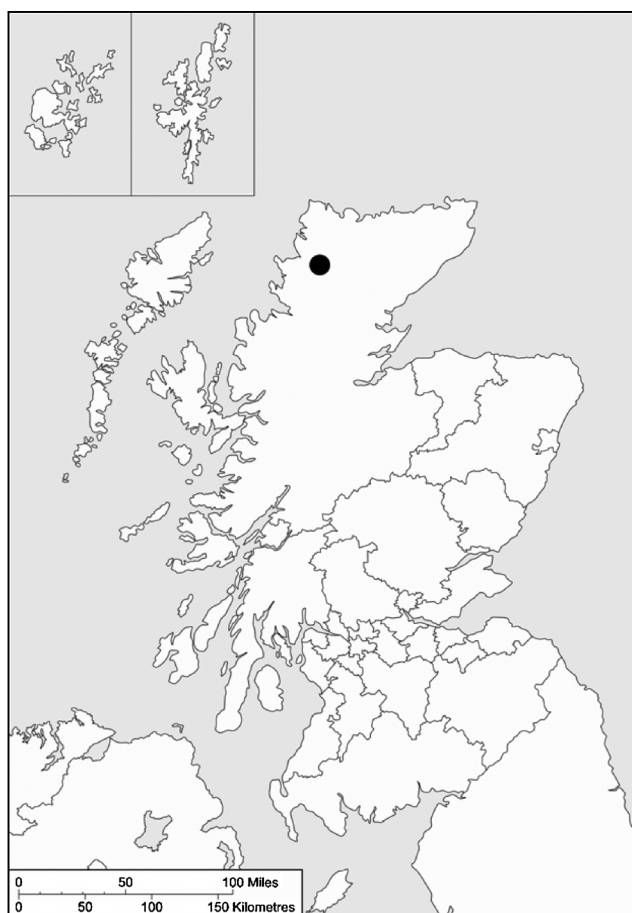


**Figure 1.** Map of Scotland showing the location of the Traligill basin.

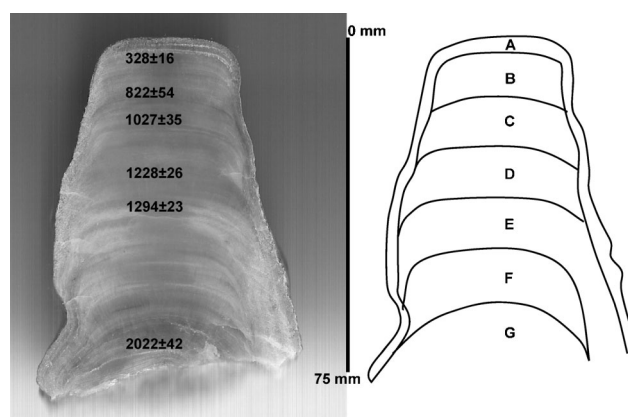


**Figure 2.** Tral-1 in section showing U–Th dates (a BP, left) and sampling scheme for lipid analysis (right).

detrital Th input and consequently correct for its presence. A standard sample bracketing technique was used for the Nu plasma to monitor and if necessary correct for drift. Two internal solution standards and one rock standard were used to assess external reproducibility. Two total procedure blanks (run in parallel with these samples) for  $^{238}\text{U}$  and  $^{232}\text{Th}$  yielded 9 and 13 pg, respectively. These blanks are negligible for the samples measured, and the apparent blank contribution for the  $^{232}\text{Th}$  concentrations of the samples is less than 1%.

### Lipid analysis

Due to the small size of the sample, for lipid analysis, one half was subsampled into seven sections (Fig. 2), using a 2-cm diamond-tipped saw, mounted on a hand-drill. The subsamples were cleaned by sonication in a 90:10 solution of dichloromethane (DCM)/methanol to remove surface contamination before further processing. Each subsample was processed by acid digestion of the calcite in 3 M cleaned hydrochloric acid, and liquid/liquid extraction of the lipids with DCM, following the protocol of Blyth *et al.* (2006). The extracts were then methylated using 3 mL boron trifluoride/methanol complex (12%  $\text{BF}_3$ /methanol; Aldrich) for 2 h at 70°C. After destruction of the  $\text{BF}_3$  complex with Milli-Q water (3 mL), and re-extraction with petroleum ether (2 mL  $\times$  6), the sample was further derivatised with five drops of BSTFA ( $\text{C}_8\text{H}_{18}\text{F}_3\text{NOSi}_2$ ; Fluka Chemika) for 2 h at 70°C, and left to stand at room temperature overnight. Cholic acid and androstanol as internal standards were added at the digestion stage to allow quantification of the lipid compounds.

Samples were analysed using a Hewlett Packard 6890 gas chromatograph split/splitless injector (at 280°C) linked to a Hewlett Packard 5973 MS detector, with the oven temperature ramped from 40 to 300°C at 4°C  $\text{min}^{-1}$ , and held at 300°C for 20 min, He as carrier gas and ionization energy of the MS set to 70 eV. The chromatograph was equipped with an HP-1MS fused silica capillary column (30 m  $\times$  0.25 mm i.d.). Initial runs were in scan mode to allow full identification of the compounds

present, but final data acquisition was in selected ion mode to maximise resolution. Lipid peaks were quantified on the appropriate ion chromatograms and calculated as  $\mu\text{g}$  ( $\text{g calcite}^{-1}$ ). They were also normalised by recalculation to a percentage of the total sum of measured lipids for each subsample to remove stalagmite growth rate artefacts.

Full process blanks were run in parallel with the sample, and showed no significant contamination of the compounds of interest.

## Results and discussion

### Stalagmite age

Stalagmite age is shown in Fig. 2 and full U–Th data are provided in Table 1. The stalagmite has very low levels of detrital thorium (7–15 p.p.b.), indicating that no further correction of the data is necessary. The basal date of the stalagmite is  $2202 \pm 42$  a, while that of the top of the main body directly below the hiatus is  $328 \pm 16$  a ( $2\sigma$  uncertainty).

### Lipid composition

Tral-1 contains saturated *n*-alkanoic acids ( $\text{C}_{12}$ – $\text{C}_{32}$ ), saturated branched alkanolic acids ( $\text{C}_{13}$ – $\text{C}_{27}$ ), mono- and di-unsaturated  $\text{C}_{18}$  alkenoic acids, *n*-alkanes ( $\text{C}_{14}$ – $\text{C}_{35}$ ), *n*-alkanols ( $\text{C}_{12}$ – $\text{C}_{30}$ ), branched alkanols ( $\text{C}_{15}$ – $\text{C}_{23}$ , odd only), sterols (cholesterol,  $\beta$ -sitosterol, stigmasterol), cholesta-3,5-dien-7-one, stigma-3,5-dien-7-one and 3-hydroxy acids ( $\text{C}_{11}$ – $\text{C}_{18}$ ). Interestingly, *n*-alkan-2-ones, reported as a major lipid component by Xie *et al.* (2003), were not identified in this sample, suggesting that their occurrence is at least partially environment-specific. Figure 3 shows example ion chromatograms from the sample.

The lipid composition shows evidence of both vegetational and microbial input, as would be expected for a deposit fed by soil water. The HMW *n*-alkanes (for the purposes of this study defined as  $\text{C}_{21}$  and above, following Xie *et al.*, 2003) show a marked odd-over-even carbon number distribution,

**Table 1.** U–Th data for Tral-1 subsamples.

	Tral-1b top	Tral-1b/c boundary	Tral-1c	Tral-1d	Tral-1e	Tral-1f	Tral-1g
$^{238}\text{U}$ (p.p.m) (uncertainty)	0.2176092 (0.0005506)	0.1947281 (0.0004320)	0.1943318 (0.0003781)	0.2037280 (0.0006943)	0.2302438 (0.0005502)	0.2183583 (0.0008385)	0.2183583 (0.0008385)
$^{234}\text{U}/^{238}\text{U}$ (uncertainty)	1.3703116 (0.0047533)	1.3785676 (0.0048514)	1.3544565 (0.0045282)	1.3660176 (0.0068425)	1.3728777 (0.0046150)	1.3643706 (0.006992)	1.3643706 (0.0069920)
$^{234}\text{U}$ (p.p.m.) (uncertainty)	0.0000161 (0.00000004)	0.0000145 (0.00000004)	0.0000142 (0.00000004)	0.0000150 (0.00000006)	0.0000171 (0.00000005)	1.608E-05 (5.781E-08)	0.0000161 (0.00000006)
$^{230}\text{Th}$ (p.p.m) (uncertainty)	1.4654E-05 (3.6076E-07)	3.2967E-05 (1.0750E-06)	4.0329E-05 (6.9372E-07)	5.0956E-05 (5.2984E-07)	6.0973E-05 (5.4841E-07)	9.742E-05 (9.183E-07)	9.7415E-05 (9.1833E-07)
$^{232}\text{Th}$ (p.p.m) (uncertainty)	0.46 (0.08)	0.59 (0.11)	1.74 (0.32)	14.78 (2.67)	9.16 (1.66)	7.26 (1.31)	7.26 (1.31)
$^{230}\text{Th}/^{232}\text{Th}$ (uncertainty)	51.9050 (2.9759)	30.8384 (2.0134)	16.5446 (0.8253)	2.2807 (0.0982)	3.9942 (0.1664)	6.9400 (0.2922)	6.9400 (0.2922)
$^{230}\text{Th}/^{234}\text{U}$ (uncertainty)	0.00300 (0.00007)	0.00750 (0.00024)	0.00936 (0.00016)	0.01119 (0.00012)	0.01178 (0.00011)	0.01998 (0.00019)	0.01998 (0.00019)
$^{234}\text{U}/^{238}\text{U}$ (uncertainty)	1.37031 (0.00475)	1.37857 (0.00485)	1.35446 (0.00453)	1.36602 (0.00684)	1.37288 (0.00462)	1.36437 (0.00699)	1.36437 (0.00699)
Age (a BP)	328	822	1027	1228	1294	2202	2202
$2\sigma$ uncertainty	$\pm 16$	$\pm 54$	$\pm 35$	$\pm 26$	$\pm 23$	$\pm 42$	$\pm 42$
Error (% 2 SEM)	4.93	6.54	3.46	2.09	1.81	1.90	1.90

SEM, standard error of mean.

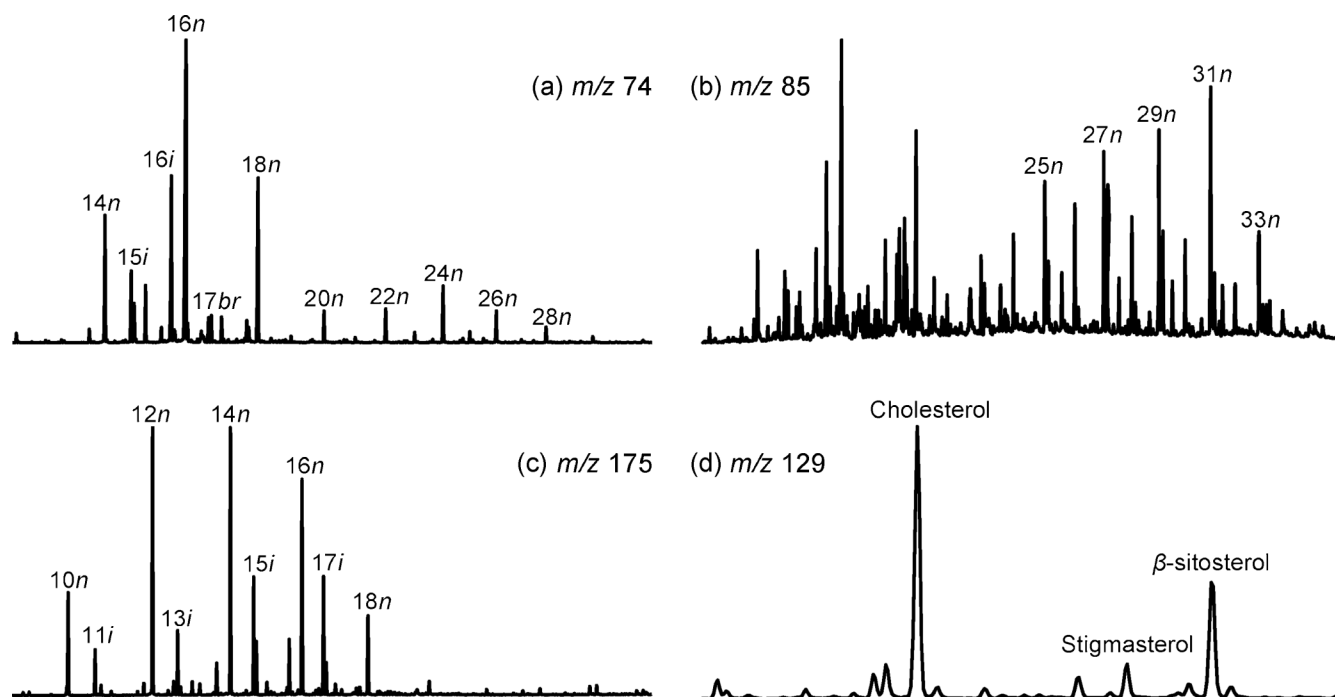


**Figure 3.** Selected ion chromatograms from subsample Tral-1a showing: (a) alkanolic acids, (b) *n*-alkanes, (c) 3-hydroxy acids and (d) sterols.

and have a carbon preference index (CPI) of between 1.7 and 4.8 (CPI<sub>2</sub>, following Marzi *et al.*, 1993), indicating a mainly but not exclusively vegetational source (Bray & Evans, 1961; Kolattukudy, 1970; Marzi *et al.*, 1993; Otto *et al.*, 1994; Marseille *et al.*, 1999). Other plant-derived markers include HMW *n*-alkanoic acids and *n*-alkanols, which show strong even-over-odd carbon predominances (Kolattukudy, 1970; Lockheart *et al.*, 2000; Bull *et al.*, 2000; Feakins *et al.*, 2007), and higher plant sterols such as stigmasterol and  $\beta$ -sitosterol (Harwood & Russell, 1984; Volkman, 1986). Specific bacterial sources are represented by the 3-hydroxy acids and the branched alkanolic acids (Kaneda, 1991; Wakeham *et al.*, 2003), whilst branched alkanols, LMW *n*-alkanoic acids, LMW *n*-alkanes, LMW *n*-alkanols and unsaturated alkanolic acids indicate more general microbial input (Cranwell, 1980; Harwood & Russell, 1984). The presence of cholesterol indicates faunal input: comparison of the stalagmite signal

with that from solvent extracts of soil samples from the top and bottom of the soil column above the cave suggests that this is predominantly derived from the conversion of plant sterols to cholesterol by soil fauna (Blyth, 2007). However, as the cave mouth is easily accessible, contributions by cave fauna and other terrestrial animals cannot be ruled out.

#### Relationships between compound groups

To investigate relationships between the different compound classes, the normalised lipid data were subjected to a principal components analysis (PCA). Two components were identified, PC1 and PC2, accounting for 63 and 20% of the variation, respectively. As can be seen from the loadings plot (Fig. 4), the compounds cluster in four distinct groups. The first, with a strongly positive score for PC1 and a negative score on PC2, consists of all the alkanes, alkanols, cholesterol and

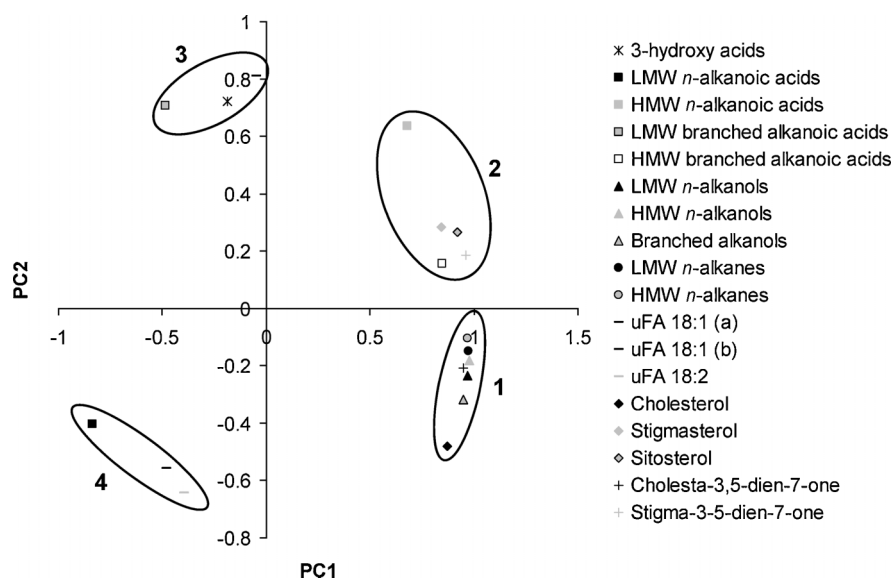


**Figure 4.** Principal components analysis loadings plot showing the relationship between the different compound groups recovered from the stalagmite. uFA, unsaturated fatty acid.

cholesta-3,5-dien-7-one. The second, related, group has an equally positive score on PC1 and a positive score on PC2 and contains the HMW alkanolic acids (normal and branched), stigmaterol,  $\beta$ -sitosterol and stigma-3,5-dien-7-one. The third group has a strongly positive score on PC2 and a negative score on PC1, and consists of the 3-hydroxy acids, the LMW branched alkanolic acids and one of the two  $C_{18}$  monounsaturated alkenoic acid isomers. The fourth group, which is negative for both PC1 and PC2, contains the LMW  $n$ -alkanoic acids and the remaining  $C_{18}$  alkenoic acids.

Group 1 contains a number of vegetation-derived compounds, as well as more general LMW microbial compounds and degradation products. The related group 2 consists primarily of plant-derived compounds. It is therefore reasonable to propose that these two groups contain the main soil-derived input to the stalagmite. Group 3 is clearly of bacterial origin, although at this stage we cannot distinguish whether this is derived from the soil or the cave bacterial communities. Group 4 may also have a microbial origin, although the generic nature of the main compounds (LMW  $n$ -alkanoic acids) prevents a robust identification.

One of the main features of these results is that the LMW aliphatic compounds previously suggested as representing

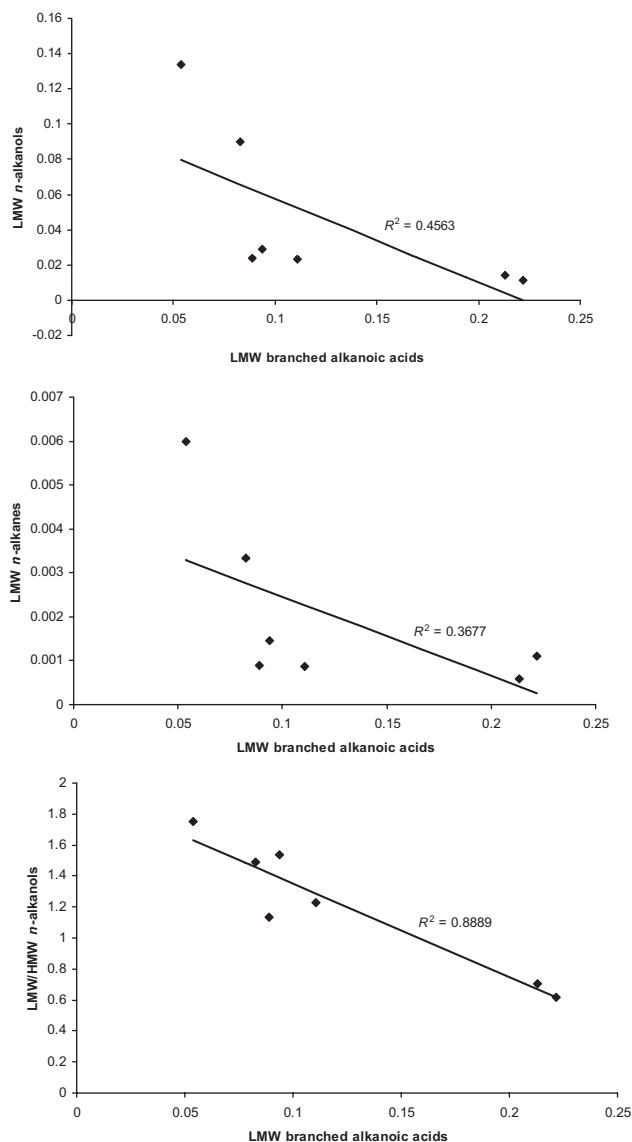


**Figure 5.** Scatter plots showing the relationship between LMW branched alkanolic acids and (from top to bottom) LMW  $n$ -alkanols, LMW  $n$ -alkanes and the ratio of LMW/HMW  $n$ -alkanols.

**Table 2.**  $r^2$  values showing the relationships (or lack thereof) between specific bacterial biomarkers (branched alkanolic acids and 3-hydroxy fatty acids) and LMW  $n$ -alkanes and  $n$ -alkanols. Negative relationships are seen between branched alkanolic acids and the  $n$ -alkanols and  $n$ -alkanes, whereas no significant relationship is seen between the 3-hydroxy acids and any other group.

Compound group 1	Compound group 2	$r^2$
Branched alkanolic acids	LMW $n$ -alkanols	-0.5
Branched alkanolic acids	LMW $n$ -alkanes	-0.4
Branched alkanolic acids	Ratio of LMW/HMW $n$ -alkanols	-0.9
Branched alkanolic acids	Ratio of LMW/HMW $n$ -alkanes	-0.7
Branched alkanolic acids	3-hydroxy acids	0.1
3-Hydroxy acids	LMW $n$ -alkanols	-0.1
3-Hydroxy acids	LMW $n$ -alkanes	-0.1

HMW, high molecular weight; LMW, low molecular weight.

bacterial activity clearly group separately from the specific bacterial biomarkers. This lack of relationship is confirmed if the normalised data are plotted as scatter plots (Fig. 5): the LMW  $n$ -alkanes and  $n$ -alkanols show a weak negative correlation ( $R^2 = -0.4$  and  $-0.5$ , respectively) with the LMW branched fatty acids. This is further supported if the LMW branched fatty acids are plotted against the ratios of LMW/HMW  $n$ -alkanols or  $n$ -alkanes, where a negative correlation ( $R^2 = -0.9$  and  $-0.7$ , respectively) is seen: this suggests that a decrease in the ratio (i.e. a decrease in the relative proportion of LMW  $n$ -alkanols and  $n$ -alkanes) corresponds to an increase in the normalised abundance of LMW branched alkanolic acids. 3-Hydroxy acids show no significant positive or negative correlation with either the  $n$ -alkanols or the  $n$ -alkanes (Table 2).

### Changes through time

The major variation in the time-series identified by the PCA is an increase in soil- and plant-derived organic matter in samples B and C. This is clearly apparent on the scores plot for the sample (Fig. 6), and in the normalised abundances of the sterols, alkanols (normal and branched, HMW and LMW, Fig. 7),  $n$ -alkanes (HMW and LMW) and HMW branched alkanolic acids. Samples B and C span a 700-year period from approximately AD 980 to AD 1680 ( $\sim 1000$ – $300$  a); this period includes the times associated with highest rainfall over the past 2 ka (Proctor *et al.*, 2000, 2002; Trouet *et al.*, 2009), and also the decrease in birch woodland (Charman *et al.*, 2001). We

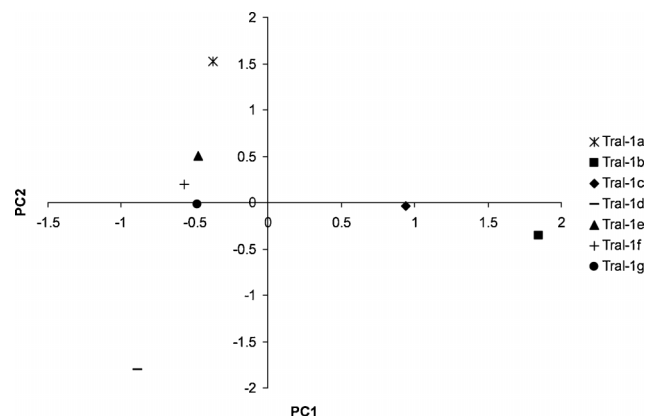


**Figure 6.** Principal components analysis scores plot showing the strongly positive score on PC1 for subsamples B and C.

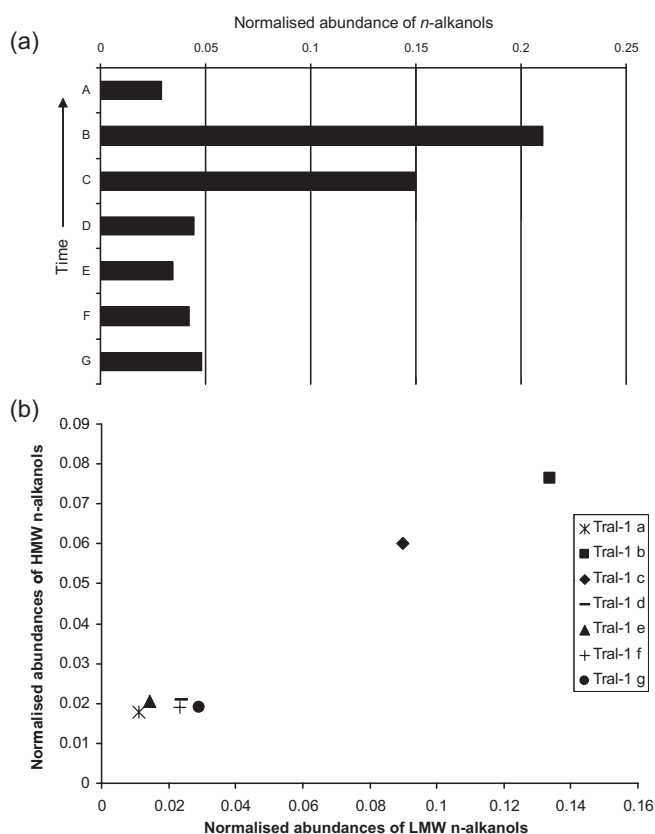


**Figure 7.** (a) Variations in the normalised abundance of *n*-alkanols through time, showing the substantial increase in subsamples B and C; (b) plot of LMW against HMW *n*-alkanols showing the concurrent increases in all chain lengths in subsamples B and C.

therefore suggest that the organic changes seen relate jointly to increased surface precipitation and soil wetness, and changes to the organic matter input and soil activity associated with a change in vegetation.

Under this hypothesis, the general increase in soil biomarkers seen in bands B and C resulted from increased throughput of organic material with increased drip-water. That this reflects an increase in input of all soil biomarkers and not a change in the amounts of plant/bacterial contribution is shown by the joint increase in both LMW and HMW compounds (Fig. 7a), and the absence of any related change in the CPI for the alkanes or alkanols. Corroborative evidence that the system feeding the stalagmite was affected by increased surface precipitation at this time comes from the change in growth rate, particularly in band B, which grew at  $500 \text{ a cm}^{-1}$ , as opposed to  $200 \text{ a cm}^{-1}$  in the lower region of the stalagmite. In samples from other caves in this area, decreased growth rate has been clearly linked to increased surface wetness (Proctor *et al.*, 2000, 2002), with soil saturation during wetter intervals resulting in a decrease in soil respiration and therefore also in the partial pressure of  $\text{CO}_2$  of the drip-water, leading to lower levels of calcite precipitation.

A change in vegetation and increase in peat formation at the base of sample C is also supported by the chain length distribution of the *n*-alkanes. Previous work on stalagmites (Blyth *et al.*, 2007) has indicated that the use of a  $\text{C}_{27}/\text{C}_{31}$  *n*-alkane ratio can distinguish between grass- and tree-dominated vegetation regimes, especially when used in combination with an overall chain length distribution plot. In this stalagmite, samples G–D have a  $\text{C}_{27}/\text{C}_{31}$  ratio of over 1, whilst samples C–A have a ratio below 1 (Fig. 8). This fits with the decline in birch woodland in the area seen in other records at around 1 ka BP. More subtle changes are apparent in the overall chain length

distribution. Band A shows a clear maximum at  $\text{C}_{31}$ , with the distribution fitting the grass-dominated regime currently extant. Band E shows a maximum at  $\text{C}_{27}$ , suggesting a particularly marked arboreal input, which is logical as the growth of band E coincides with the maximum abundance of birch pollen in the locality (Charman *et al.*, 2001), while bands B, C, D, F and G all have maxima at  $\text{C}_{25}$ .  $\text{C}_{25}$  *n*-alkane, along with  $\text{C}_{23}$ , has previously been identified as a potential biomarker for peat, and especially *Sphagnum* (Pancost *et al.*, 2002); interestingly, the two samples, A and E, that do not show maxima at  $\text{C}_{25}$ , are also the two samples with the lowest relative proportions of  $\text{C}_{23}$ . Based on these data, we suggest that the area of the cave catchment has seen five vegetation phases during the 2 ka that the stalagmite formed: during bands G and F, birch woodland dominated with some peat present (indicated by high relative abundances of  $\text{C}_{25}$  and  $\text{C}_{23}$ , and a  $\text{C}_{27}/\text{C}_{31}$  ratio  $>1$ ); this gave way to a tree-dominated regime during band E (indicated by the  $\text{C}_{27}/\text{C}_{31}$  ratio, and a chain length maximum at  $\text{C}_{27}$ ); during band D there was a return to a mixed birch and peat regime (demonstrated by an alkane distribution clearly dominated by  $\text{C}_{25}$ , but with the highest  $\text{C}_{27}/\text{C}_{31}$  ratio); this was followed by a total loss of birch, and a move to a more open peat-dominated regime in bands B and C (indicated by the chain length maximum at  $\text{C}_{25}$ , and a  $\text{C}_{27}/\text{C}_{31}$  ratio  $<1$ ); and this ultimately gave way to non-peaty mineral soils and grassland in band A. We suggest that the last of these changes, which seems to be associated with a number of hiatuses in the stalagmite, was probably caused by the earlier loss of trees leading to slope destabilisation above the cave, which, combined with extreme weather events associated with the Little Ice Age in the area, resulted in major soil loss. This would account for both the hiatuses themselves and for the change from the peaty conditions apparent earlier in the sample to the thin mineral soils seen today.

A second set of changes in the biomarker record through time is associated with bands E and A, which as well as the above-mentioned changes in *n*-alkane distribution, also reveal a decrease in the LMW/HMW *n*-alkanol and *n*-alkane ratios (in favour of HMW compounds - this is particularly marked in the *n*-alkanols where the ratio falls below 1 in these two samples; see Fig. 9), and a relative increase in LMW branched fatty acids. We suggest that this change is also principally related to surface precipitation and soil moisture. As discussed above, the changes in *n*-alkane distribution indicate a decrease in peat input in favour of arboreal vegetation in band E, and a loss of peat altogether in band A. By extension, this also indicates drier soils. A less water-saturated soil environment will promote both organic matter degradation and microbial activity within the soil, the former resulting in a relative decrease in LMW compounds, as they degrade more quickly than their HMW homologues, and the latter in an increase in bacterial biomarkers as represented by the LMW branched fatty acids. At this stage it is not possible to say whether this is a result of drier climate or, particularly in the case of band A, increased desiccation of the soils due to previous soil and vegetation loss.

Figure 10 presents a summary of our interpretation of the environmental changes through time.

### Utility of different lipid proxies

These results suggest that lipid biomarker records in stalagmites do reflect clear changes in the overlying environment, with the use of *n*-alkane distributions, and especially the  $\text{C}_{27}/\text{C}_{31}$  ratio, to interpret changes in vegetation regime being particularly successful. This proxy has now been applied with consistent results to stalagmites from China (Xie *et al.*, 2003), Ethiopia

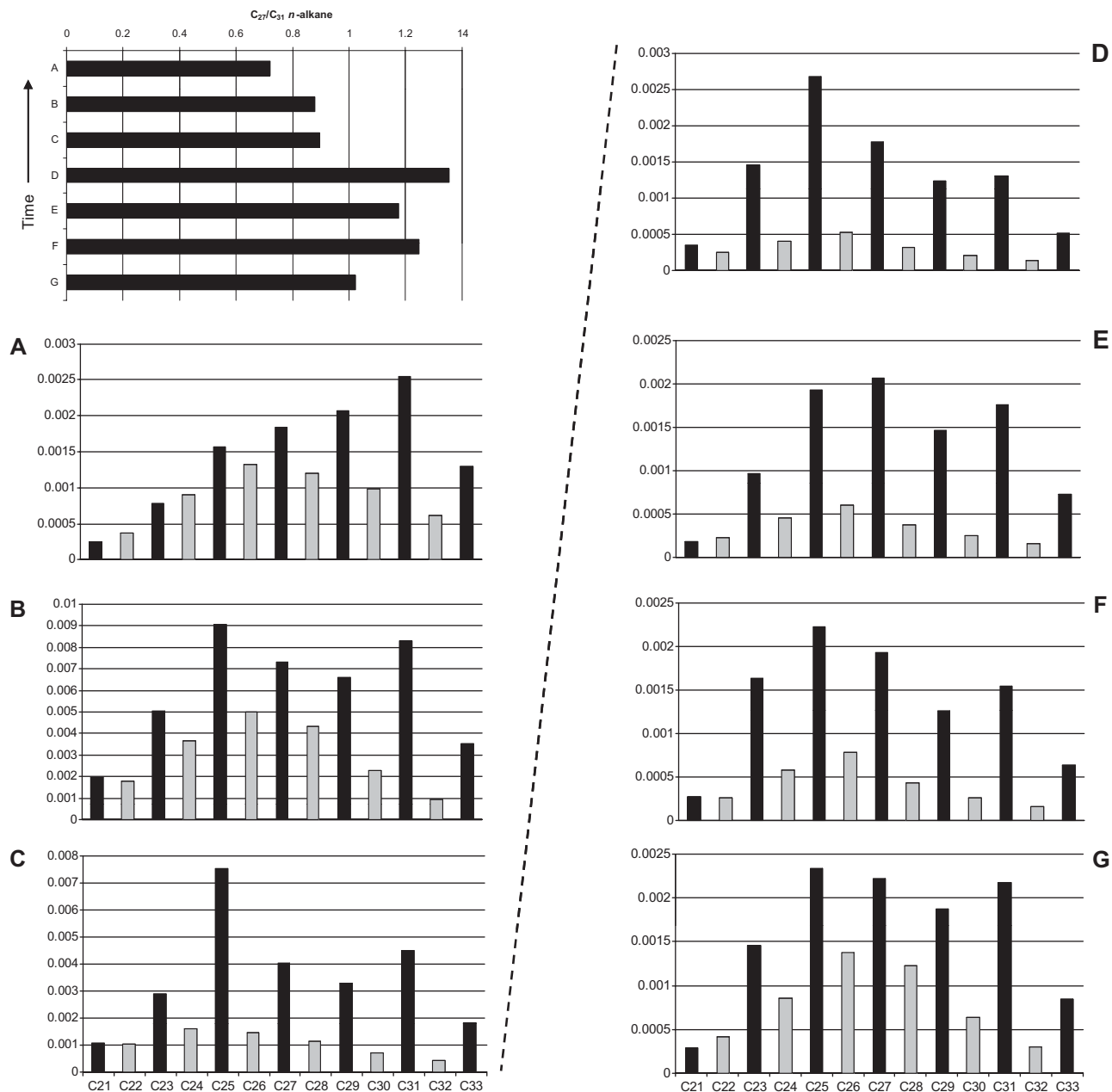


**Figure 8.** (Top left) Variations in the ratio of  $C_{27}/C_{31}$  *n*-alkanes through time. (A–G) Changes in the carbon number distribution of HMW *n*-alkanes through time. Odd number compounds are shown in black, even numbers in grey.

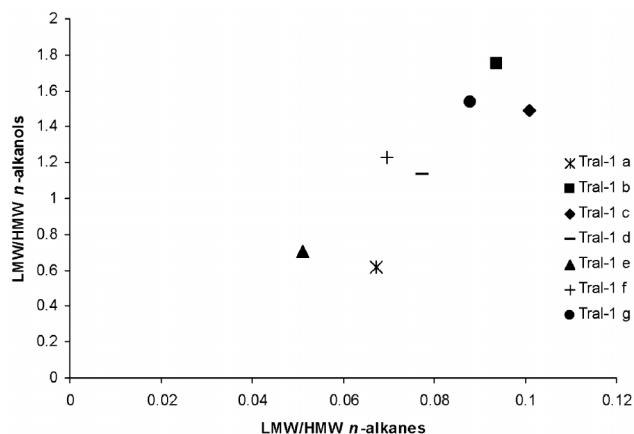


**Figure 9.** Scatter plot of LMW/HMW *n*-alkanols against LMW/HMW *n*-alkanes showing the decrease in both ratios in subsamples A and E.

(Blyth *et al.*, 2007) and Scotland, and given the contrasting range of climates, timescales and soil environments involved in the different studies, we have no reason to believe that it will not be equally applicable elsewhere.

Interpreting changes in soil environment and their relationship with climate is less clear cut. Xie *et al.* (2003) showed a coherent relationship between North Atlantic sea surface temperature and ratios of LMW/HMW *n*-alkanols and *n*-alkan-2-ones, which was interpreted as reflecting fluctuations in the relative amounts of vegetational and microbial input to the soil, driven by temperature. The magnitude of these lipid changes and their relationship to global climate is not in doubt. However, the work here suggests that the controls on changes in these ratios are complex, and may relate as much to selective compound degradation as organic matter source. In particular, no evidence was found to link the abundance of LMW compounds directly with bacterial activity, with an inverse relationship in fact being seen between the relative abundances of LMW *n*-alkanols and *n*-alkanes and the abundance of

	Vegetation, indicated by <i>n</i> -alkane distribution	Soil conditions
0 a		
A	Grass over thin mineral soils	Drier soils destabilised by vegetation loss
328 ± 16 a		
B	Open peat	High surface precipitation rates leading to a higher rate of transport of fresh organic matter from soil to cave, and a decrease in stalagmite growth
822 ± 54 a		
C	Peat cover increases, birch lost	Increasing surface and soil wetness, and OM input
1027 ± 35 a		
D	Mixed birch and peat	
1228 ± 26 a		
E	Birch woodland	Drier soil conditions indicated
F		
G	Birch dominated, but with some peat	
2022 ± 42 a		

**Figure 10.** Summary of palaeoenvironmental history as recorded by the lipid composition of Tral-1.

LMW branched fatty acids, which are known bacterial biomarkers.

The use of fatty acids as environmental markers in stalagmites is currently unproven. The only notable change in the *n*-fatty acids in this stalagmite is a decrease in the normalised abundance of the HMW homologues in band D. Blyth *et al.* (2007) attributed increases in HMW fatty acids in an Ethiopian sample to increased plant matter input to the soil during agricultural processes. However, agriculture is not a potential control at this site, and, unlike in the Ethiopian sample, the change in fatty acid abundance does not correlate with changes in other markers for vegetation input such as relative abundance of HMW *n*-alkanols and *n*-alkanes, suggesting that a simple change in vegetation input is unlikely to be the main driver for this record.

A second change in fatty acids in band D occurs in the ratio of unsaturated to saturated C<sub>18</sub> acids, with an increase being seen in the C<sub>18:2</sub> compound, and one of the two C<sub>18:1</sub> isomers (the second C<sub>18:1</sub> isomer does not show any related fluctuations through time; see Fig. 11). Xie *et al.* (2005) found that increases in the ratio of monounsaturated to saturated C<sub>16</sub> and C<sub>18</sub> fatty acids in a Chinese stalagmite coincided with the North Atlantic Heinrich event (H1), and hypothesised that this reflected a combination of an increase in unsaturated fatty acid synthesis due to temperature-driven metabolic changes in the bacteria, and decreased degradation due to lower biological activity in colder periods. However, the record did not reflect other major climatic events such as the last glacial maximum, Younger Dryas or Bølling-Allerød. Of particular note in the current sample is that although two unsaturated acids show coincident changes in band D, the second monounsaturated isomer does not display similar variations, and instead shows a significant increase in band A (Fig. 11). This suggests that in using unsaturated fatty acids to judge whether environmental change has occurred it is necessary to know which isomers are affected, and which are being measured. To our knowledge this is not an issue that has been explored in this context.

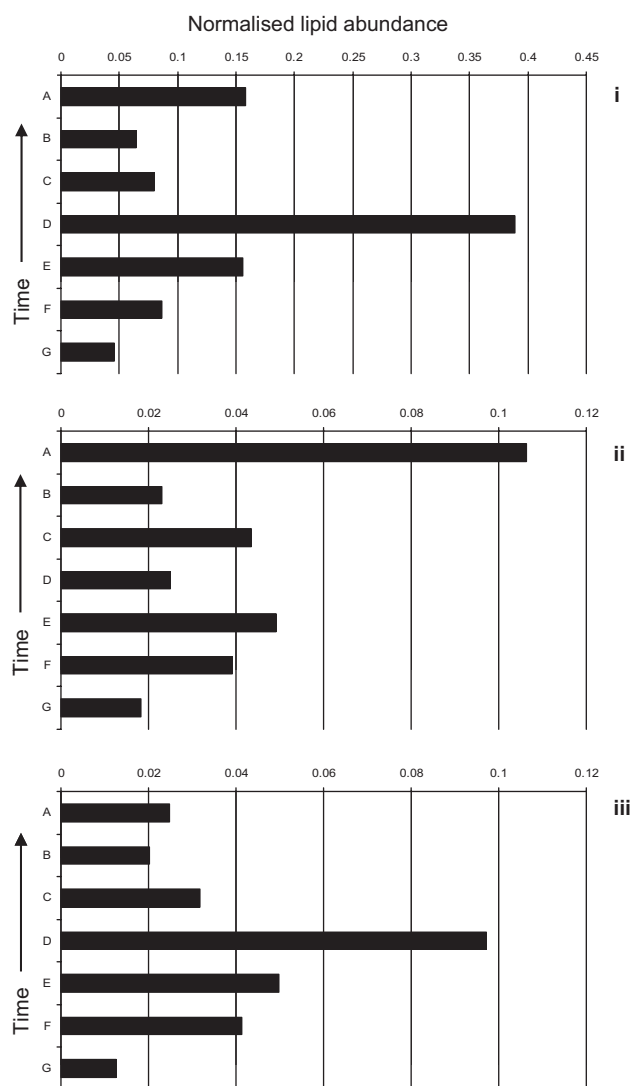


**Figure 11.** Bar charts showing the variation through time in two C<sub>18:1</sub> alkanolic acid isomers (a and b) and the C<sub>18:2</sub> alkanolic acid (c).

One major factor in determining changes in particular proxies will be the primary limiting climatic factor on the soil. In north Scotland over the past 2 ka, the soils are clearly precipitation-limited (Proctor *et al.*, 2000, 2002), with the degree of saturation affecting both biological activity and compound degradation. In other areas, or on different time scales, temperature may be the limiting factor. The source of the lipids will also affect whether temperature or precipitation is the more important control, with bacterial lipids sourced from in-cave environments likely to be seen to respond more to temperature than to surface precipitation (if water flow falls to a degree unable to feed the microbial communities, it is highly unlikely the stalagmite will be growing), while soil bacteria and vegetation will be subject to a more complex series of controls.

## Conclusion

This study analysed the lipid biomarker records preserved in a 2 ka stalagmite record from north-west Scotland, with the aim of testing the wider applicability of potential environmental proxies previously identified. When viewed in the context of published studies (Xie *et al.*, 2003, 2005; Blyth *et al.*, 2007, 2008) it is clear that some proxies are applicable to a wide range of areas, environments and time scales. In particular, the



use of the *n*-alkane C<sub>27</sub>/C<sub>31</sub> ratio and chain length distributions has now been applied successfully in Scotland, Ethiopia (Blyth *et al.*, 2007) and China (Xie *et al.*, 2003), and may be considered relatively robust in this context, provided they are not used indiscriminately. We have shown that it is also possible to interpret basic climatic parameters and changes in soil conditions and organic matter decomposition, although this was most successfully achieved by a holistic examination of changes across the whole lipid composition and not the formation of a compound-specific proxy. Indeed, for some previously proposed lipid proxies (e.g. HMW versus LMW ratios; *n*-alkanoic acid abundances and ratios), the controls on lipid abundance in speleothems (input of different organism groups, compound degradation, etc.) and their relationship with different climatic drivers (temperature, surface precipitation) are currently less well elucidated. In particular, the contribution of bacteria is complicated by having dual potential sources, being both derived from the soil, and *in situ* cave microbial communities. We therefore recommend that these lipid parameters should be studied in stalagmites, but caution and consideration of the likely climatic limiting factors on the area should be applied in interpretation. Further work investigating the main sources of microbial input in stalagmites and transport of organic matter between soil and cave will clarify many of these issues, allowing a fuller range of lipid proxies in stalagmites to be revisited in future.

**Acknowledgements.** The analytical phase of this work was supported by an NERC studentship to A.J.B. (NER/S/A/2003/11297), and fieldwork was supported by NERC RAPID funding to A.B. Paul Donohue of the School of Civil Engineering and Geosciences, Newcastle University, provided analytical support, and Sam Hammond (Department of Earth & Environmental Sciences, the Open University) is thanked for her technical support in the U–Th dating. Figure 1 was drawn by Kevin Burkhill of the University of Birmingham, who is gratefully acknowledged.

**Abbreviations.** CPI, carbon preference index; DCM, dichloromethane; HMW, high-molecular-weight; LMW, low-molecular-weight; MS, Mass Spectrometer; PCA, principal components analysis.

## References

- Baker A, Caseldine CJ, Gilmour MA, *et al.* 1999. Stalagmite luminescence and peat humification records of palaeo-moisture for the last 2500 years. *Earth and Planetary Science Letters*, **165**: 157–162.
- Blyth AJ. 2007. *Lipid biomarkers in speleothems*. PhD thesis, University of Newcastle Upon Tyne.
- Blyth AJ, Frisia S. 2008. Molecular evidence for bacterial mediation of calcite formation in cold high-altitude caves. *Geomicrobiology Journal* **25**: 101–111.
- Blyth AJ, Farrimond P, Jones DM. 2006. An optimised method for the extraction and analysis of lipid biomarkers from stalagmites. *Organic Geochemistry*, **37**: 882–890.
- Blyth AJ, Asrat A, Baker A, *et al.* 2007. A new approach to detecting vegetation and land-use change using high resolution lipid biomarker records in stalagmites. *Quaternary Research* **68**: 314–324.
- Blyth AJ, Baker A, Penkman KEH, *et al.* 2008. Molecular organic matter in speleothems as an environmental proxy. *Quaternary Science Reviews* **27**: 905–921.
- Bray EE, Evans ED. 1961. Distribution of *n*-paraffins as a clue to recognition of source beds. *Geochimica et Cosmochimica Acta* **22**: 2–15.
- Bull ID, van Bergen PF, Nott CJ, *et al.* 2000. Organic geochemical studies of soils from the Rothamsted classical experiments – V. The fate of lipids in different long-term experiments. *Organic Geochemistry*, **31**: 389–408.
- Charman DJ, Caseldine C, Baker A, *et al.* 2001. Palaeohydrological records from peat profiles and speleothems in Sunderland, Northwest Scotland. *Quaternary Research*, **55**: 223–234.
- Cranwell PA. 1980. Branched/cyclic alkanols in lacustrine sediments (Great Britain): recognition of *iso*- and *anteiso*-branching and stereochemical analysis of homologous alkan-2-ols. *Chemical Geology* **30**: 15–26.
- Dowswell P. 1988. Caves of the Traligill Basin. In: T.J. Lawson (ed.) The limestone caves of Scotland, part 2: Caves of Assynt. *The Grampian Speleological Group Occasional Publication*, No. 6 25–40.
- Edwards RL, Chen JH, Wasserburg GJ. 1987. <sup>238</sup>U–<sup>234</sup>U–<sup>232</sup>Th–<sup>230</sup>Th systematics and the precise measurement of time over the last 500,000 years. *Earth and Planetary Science Letters* **81**: 175–192.
- Feakins SJ, Eglinton TI, deMenocal PB. 2007. A comparison of biomarker records of northeast African vegetation from lacustrine and marine sediments (ca. 3.40 Ma). *Organic Geochemistry* **38**: 1607–1624.
- Harwood JL, Russell NJ. 1984. *Lipids in plants and microbes*. George Allen & Unwin: London.
- Huang X, Cui J, Pu Y, *et al.* 2008. Identifying ‘free’ and ‘bound’ lipid fractions in stalagmite samples: an example from Heshang Cave, Southern China. *Applied Geochemistry* **23**: 2589–2595.
- Kaneda T. 1991. *Iso*- and *anteiso*-fatty acids in bacteria: biosynthesis, function, and taxonomic significance. *Microbiological Reviews* **55**: 288–302.
- Kolattukudy PE. 1970. Plant waxes. *Lipids* **5**: 259–275.
- Lockheart MJ, van Bergen PF, Evershed RP. 2000. Chemotaxonomic classification of fossil leaves from the Miocene Clarkia lake deposit, Idaho, USA based on *n*-alkyl lipid distributions and principal component analyses. *Organic Geochemistry* **31**: 1223–1246.
- Marseille F, Disnar JR, Guillet B, *et al.* 1999. *n*-Alkanes and free fatty acids in humus and A1 horizons of soils under beech, spruce and grass in the Massif-Central (Mont-Lozère), France. *European Journal of Soil Science* **50**: 433–441.
- Marzi R, Torkelson BE, Olson RK. 1993. A revised carbon preference index. *Organic Geochemistry* **20**: 1303–1306.
- McDermott F. 2004. Palaeo-climate reconstruction from stable isotope variations in speleothems: a review. *Quaternary Science Reviews* **23**: 901–918.
- Otto A, Walther H, Puttmann W. 1994. Molecular composition of a leaf- and root-bearing Oligocene oxbow lake clay in Weisshelster Basin, Germany. *Organic Geochemistry* **22**: 275–286.
- Pancost RD, Baas M, van Geel B, *et al.* 2002. Biomarkers as proxies for plant inputs to peats: an example from a sub-boreal ombrotrophic bog. *Organic Geochemistry* **33**: 675–690.
- Proctor CJ, Baker A, Barnes WL, *et al.* 2000. A thousand year speleothem proxy record of North Atlantic climate from Scotland. *Climate Dynamics* **16**: 815–820.
- Proctor CJ, Baker A, Barnes WL. 2002. A three thousand year record of North Atlantic climate. *Climate Dynamics* **19**: 449–454.
- Trouet V, Esper J, Graham NE, *et al.* 2009. Persistent positive North Atlantic Oscillation mode dominated the Medieval Climate Anomaly. *Science* **324**: 78–80.
- Turner S, van Calsteren P, Vigier N, *et al.* 2001. Determination of thorium and uranium isotope ratios in low-concentration geological materials using a fixed multi-collector MC-ICP-MS. *Journal of Analytical Atomic Spectrometry* **16**: 612–615.
- Volkman JK. 1986. A review of sterol markers for marine and terrigenous organic matter. *Organic Geochemistry* **9**: 83–99.
- Wakeham SG, Pease TK, Benner R. 2003. Hydroxy fatty acids in marine dissolved organic matter as indicators of bacterial membrane material. *Organic Geochemistry* **34**: 857–868.
- Xie S, Yi Y, Huang J, *et al.* 2003. Lipid distribution in a subtropical southern China stalagmite as a record of soil ecosystem response to palaeoclimate change. *Quaternary Research* **60**: 340–347.
- Xie S, Huang J, Wang H, *et al.* 2005. Distributions of fatty acids in a stalagmite related to palaeoclimate change at Qingjiang in Hubei, southern China. *Science in China Series D Earth Sciences* **48**: 1463–1469.